Supporting Information for:

Solar-Driven Reduction of 1 atm CO_2 to Formate at 10% Energy-Conversion Efficiency by Use of a TiO_2-Protected III-V Tandem Photoanode in Conjunction with Bipolar Membrane and a Pd/C Cathode Electrocatalyst

Xinghao Zhou[1,2], Rui Liu[2], Ke Sun[2,3], Yikai Chen[2], Erik Verlage[1,2], Sonja A. Francis[2-4], Nathan S. Lewis[2,3,5,6], Chengxiang Xiang[2,3*]*

[1] Division of Engineering and Applied Science, Department of Applied Physics and Materials Science, California Institute of Technology, Pasadena, CA 91125, USA

[2] Joint Center for Artificial Photosynthesis, California Institute of Technology, Pasadena, CA 91125, USA

[3] Division of Chemistry and Chemical Engineering, California Institute of Technology, Pasadena, CA 91125, USA

[4] Resnick Sustainability Institute, California Institute of Technology, Pasadena, CA 91125, USA

[5] Beckman Institute and Molecular Materials Research Center, California Institute of Technology, Pasadena, CA 91125, USA

[6] Kavli Nanoscience Institute, California Institute of Technology, Pasadena, CA 91125, USA

*To whom correspondence should be addressed: nslewis@caltech.edu, cxx@caltech.edu

Chemicals and materials

All materials were used as received unless noted otherwise: potassium hydroxide pellets (KOH, Macron Chemicals, ACS 88%), 10 wt.% Pd on Vulcan XC-72 carbon black (Pd/C, Premetek Co.), titanium wire (Ti wire, Alfa Aesar, 99.7%), CO_2 gas (ALPHAGAZ 1), and 10 wt.% Nafion (Sigma-Aldrich). Water with a resistivity > 18 MΩ-cm was obtained from a Barnsted Nanopure deionized (DI) water system. The $KHCO_3$ solution was prepared by vigorously bubbling CO_2(g) through K_2CO_3 solutions until the pH did not change. The bipolar membrane (fumasep® FBM) was obtained from FuMA-Tech GmbH (St. Ingbert, Germany) and was stored in 1.0 M NaCl(aq) at room temperature. The bipolar membrane (BPM) was cut into 1.5×1.5 cm pieces and rinsed with H_2O before use. Nafion® PFSA 117 membrane (Chemours) with a thickness of 183 μm was obtained from Dupont. The Nafion was soaked in H_2O for > 4 h and rinsed with H_2O before use.

Growth of III-V dual junction photoabsorbers

The tandem-junction III-V device was grown commercially (Sumika Electronic Materials, Inc.) according to specifications determined by 1-D numerical simulation using Helmholtz-Zentrum Berlin's AFORS-HET software. Planar III-V layers were grown epitaxially by metal-organic chemical-vapor deposition (MOCVD) on an n^+-GaAs wafer that had a (100)-oriented polished surface (Si-doped, acceptor concentration of 1×10^{19} cm^{-3}, 6" diameter). Detailed information on the cell stack, including the thickness and the dopants for the III-V layers, has been provided previously.[1]

Atomic-layer deposition of TiO_2 layer

Atomic-layer deposition (ALD) of TiO_2 was conducted at 150 °C using tetrakis(dimethylamido)titanium (TDMAT, Sigma-Aldrich, 99.999%, used as received) and H_2O (>18.2 MΩ-cm resistivity, Millipore) in an Ultratech Fiji 200 plasma atomic-layer deposition system. Prior to ALD, the epitaxial surface was immersed in 1.0 M KOH(aq) (aqueous solution

of potassium hydroxide pellets, semiconductor grade, 99.99% trace metal basis, Sigma-Aldrich) for 30 s, rinsed with copious amounts of H_2O, dried using a stream of N_2(g), and loaded immediately into the ALD chamber. An ALD cycle consisted of a 0.06 s pulse of H_2O, a 15 s purge under a constant 0.13 L min^{-1} flow of research-grade Ar(g), a 0.25 s pulse of TDMAT, and another 15 s Ar(g) purge. ALD-TiO_2 films with thickness of 62.5 nm were used to protect III-V surfaces.

Ohmic contacts and deposition of Ni

Ohmic contact to the n^+-GaAs wafer was formed using a Ge-Au eutectic (20 nm Ge/ 30 nm Au/ 15 nm Ni/ 100 nm Au) deposited by radio-frequency (RF) sputtering. The contact layers were annealed under N_2(g) at 400 °C for 30 s using rapid thermal annealing (RTA) with a ramp-up rate of 40 °C s^{-1}. For all photoanode surfaces, an optically transparent nominally 2 nm thick Ni film was deposited on TiO_2 via RF sputtering from a Ni target (Kurt Lesker, 2'' diameter × 0.125'' thickness, 99.95%) using an AJA high-vacuum magnetron sputtering system. The Ar flow was kept at 10 sccm, while the working pressure was held at 5 mTorr. A deposition rate of ~0.1 Å s^{-1} was maintained by adjusting the sputtering power on the Ni target.

ALD-deposited amorphous TiO_2 coatings have been used on various single crystalline substrates, including Si, III-V and II-VI compound semiconductors previously, and have showed excellent ohmic behavior due to similar growth chemistry. Degenerately doped Si substrates with an acceptor concentration > $10^{19}cm^{-3}$ p^+-Si were used in this study as the dark electrode control sample, to be consistent with the actual sample that had a window layer consisting of a 30-nm p^+-$In_{0.48}Al_{0.57}P$ and a 7-nm thick p^+-GaAs with acceptor concentrations > 10^{19} cm^{-3}. The tandem III-V n-type photoelectrode was rectifying in the dark and therefore could not be used as a reliable reference for the behavior of the photoelectrode under illumination.[2] The J-E behavior of the p^+-Si/TiO_2/Ni dark electrode effecting the OER in 1.0 M KOH(aq) thus provided a measure of the OER overpotential properties of the Ni-containing catalyst on a relevant substrate.

Preparation of Pd/C electrodes

The preparation of electrodes comprising Pd/C on a Ti mesh was similar to that reported previously for Pd/C on a Ti foil electrode.[3] A Ti mesh was first cut into 0.04 cm^2 pieces. Five pieces of Ti mesh were stacked and stringed together with a Ti wire. The stacked Ti mesh was etched in boiling 10% oxalic acid, rinsed thoroughly with H_2O, and dried overnight 75 °C in an oven. 4.8 mg of Pd/C powder was then mixed with 2.4 ml isopropanol and 40 µL 10 wt.% Nafion and the mixture was sonicated for > 30 min. The resulting solution was drop-dried onto the Ti mesh, with a Pd mass loading of 250 µg cm^{-2}. The Pd mass loading of Pd/C coated Ti foil reported previously was 50 µg cm^{-2}. As a comparison, a Pd/C nanoparticle-coated Ti foil electrode was made using the same conditions as on the Ti mesh except that the Pd mass loading was 50 µg cm^{-2}.

Preparation of III-V dual junction photoanodes

The ohmically contacted tandem-junction wafers were cleaved into samples that were ~0.1 cm^2 area. Ag paste was then used to attach the ohmic contact to a coiled, tin-plated Cu wire (McMaster-Carr) which was then threaded through a glass tube (Corning Inc., Pyrex tubing, 7740 glass). The samples were encapsulated and sealed to the glass tube using grey epoxy (Hysol 9460F). The epoxy was allowed to dry under ambient pressure for > 12 h. The exposed electrode surfaces were imaged with a high-resolution optical scanner (Epson perfection V370 with a resolution of 2400 dpi) and the areas were measured using ImageJ software. Electrodes were ~ 0.03 cm^2 in photoactive area unless specified otherwise.

3-electrode measurements

For electrochemical measurements in 2.8 M $KHCO_3$(aq), a Ag/AgCl/1.0 mol/kg KCl electrode was used as the reference electrode, and a Pt mesh was used as the counter electrode. The Ag/AgCl/1.0 mol kg^{-1} KCl electrode had a potential of 0.235 V vs the normal hydrogen electrode (NHE). The pH of the CO_2-saturated 2.8 M $KHCO_3$(aq) solution was 8.0, as measured

by a VWR SympHony SB70P Digital, Bench-model pH Meter. The equilibrium potential for the CO_2/HCO_2^- redox couple at pH 8 is 0.02 V versus the reversible hydrogen electrode (RHE).[4] Therefore, the equilibrium potential for CO_2 reduction to formate in CO_2-saturated 2.8 M $KHCO_3$(aq) solution was calculated to be -0.687 versus Ag/AgCl/1.0 mol kg^{-1} KCl.

Figure S2A shows the configuration of 3-electrode electrochemical measurement. Two custom-made three-necked cells were used in the 3-electrode measurement. The BPM was used for prevention of formate product cross-over, and to prevent the formate from being oxidized at the counter electrode. The electrolyte was vigorously agitated with a magnetic stir bar driven by a model-train motor (Pittman) with a Railpower 1370 speed controller (Model Rectifier Corporation). The data presented for electrochemical measurements in aqueous solutions do not include compensation for the series resistance of the solution. CO_2(g) was bubbled into the $KHCO_3$ solution during electrochemical measurements, to prevent oxygen dissolution. Cyclic voltammetric data (10 mV s^{-1} scan rate) were obtained with a Biologic MPG-2-44 potentiostat (Bio-Logic Science Instrument).

2-electrode measurements

The configuration for 2-electrode measurements was similar to that used to obtain 3-electrode measurements (Figure S2B). In addition to the stirring described above, a peristaltic pumping system (Simply Pumps PM300F) with a minimum flow rate of 500 mL min^{-1}, as controlled by a tunable power supply, was used to facilitate the removal of CO_2 bubbles at the BPM surface, and to minimize the voltage loss at the BPM caused by bubbles. The BPM in this configuration was replaced as required by a Nafion membrane for additional 2-electrode measurements. For photoelectrochemical experiments, a Xe arc lamp (Newport 67005 and 69911) equipped with an IR filter (Newport 61945) and with an AM 1.5 filter (Newport 81094 and 71260) was used as the light source for *J-E* measurements. The intensity in the solution-containing cell was then calibrated by placing a Si photodiode (FDS100-Cal, Thorlabs) with a similar area as that of the photoanode (0.03 cm^2) in the custom-made three-necked beaker with

flat quartz windows, with the Si located at nominally the same position as that occupied by the exposed area of the photoelectrode. The Si photodiode had been previously calibrated by measurement of the short-circuit current density under 100 mW cm^{-2} of AM 1.5 simulated sunlight. The voltage scan range was confined to be more positive than the onset of photoanodic current, to ensure a constant direction of ionic current flow in the membrane. The areas for the photoanode, BPM, Nafion membrane and Pd/C cathode were 0.03 cm^2, 0.03 cm^2, 0.03 cm^2, 0.04 cm^2, respectively. A 0.2 cm diameter hole was punched at the middle of a piece of rubber using a hole making tool. An O-ring with 0.2 cm diameter was glued with epoxy on the rubber with the hole aligned. The BPM was right between two pieces of rubber, and the hard rubber/O-ring/BPM/O-ring/hard rubber was tightly clamped between the two cells as shown in Figure S2B.

Four-point measurement system for the bipolar membrane

The four-point measurement setup was similar to that used for the 2-electrode measurement (Figure S2C). Two Luggin capillaries with Ag/AgCl/1.0 mol kg^{-1} KCl reference electrodes were used to measure the potential near the membrane. A peristaltic pumping system was also used in these experiments to facilitate the removal of CO_2 bubbles from the BPM surface, and to minimize the voltage loss at the BPM caused by bubbles and concentration gradients. The BPM in this configuration could be replaced by Nafion membrane as appropriate for four-point measurements of the Nafion membrane. The voltage loss at 10 mA cm^{-2} was lower than previously measured,[5] due to the use of Luggin capillaries as well as an efficient pumping system.

ICP-MS potassium ion crossover measurements

To measure the potassium ion crossover from the anolyte to the catholyte through the BPM, the $KHCO_3$ catholyte was replaced by $CsHCO_3$ (Sigma-Aldrich, 99.9% trace metals basis). Two Pt mesh electrodes were used as the source and drain electrodes during the potassium ion crossover tests. The potassium ion concentrations in the catholyte in a 2-electrode BPM

configuration were determined as a function of time by Inductively Coupled Plasma – Mass Spectrometry using an Agilent 8800 spectrometer. The sample-introduction system consisted of a MicroMist nebulizer with a Scott-type spray chamber. A fixed-injector quartz torch was used with a guard electrode, and the plasma was operated at 1500 W. In addition to use of single-quad (MS) mode with no gas, elements were determined by MS-MS modes in which different collision or reactive gases were present in the gas cell located between the quadrupoles. These modes were no-gas, He, H. External standards were used to quantify the analytes determined.

TIC/TOC carbonate ion crossover measurements

To measure the carbonate ion crossover from the catholyte to the anolyte through the BPM, the anode chamber was sealed and purged with O_2(g) (ALPHAGAZ 1) to prevent sorption of CO_2(g) from ambient air. Samples were analyzed for total inorganic carbon (TIC) using an OI Analytical Aurora Total Organic Carbon Analyzer. Briefly, a sample aliquot was combined with phosphoric acid and heated in a closed vessel. At the end of the reaction time, carbon dioxide was swept out of the vessel by a purge of N_2(g). The gas stream was dried and passed through a non-dispersive infrared (NDIR) detector. The instrument was calibrated against potassium hydrogen phthalate that had been oxidized to form carbon dioxide by heating persulfate, after removal of TIC as described above. For these experiments, the instrument was calibrated and showed a linear response between 5 and 50 ppm.

Faradaic efficiency for formate generation

^{1}H NMR spectroscopy was performed on a Bruker 400 MHz Spectrometer to quantify the amount of formate generation. Standards of 40 to 500 μM sodium formate solutions were prepared by serial dilution, and were used to calibrate the instrument (Figure S7). In general, 100 μL of 0.0800 vol.% 1,1'-dimethylformamide, DMF (internal standard), in H_2O were added to a 2 mL aliquot of the standard solution. 0.5 mL of this solution was then transferred to a NMR tube that contained 200 μL of D_2O. A water suppression method was used to suppress the

signal of the water in the electrolyte and to allow visualization of the formate peaks. The same procedure was used to quantify the formate product, with 100 μL of 0.0800 vol.% DMF solution added to 2 mL of the electrolyte after electrolysis, and 0.5 mL of the solution added in a NMR tube with 200 μL of D_2O.

Discussion of nickel catalyst

The catalysts are denoted as Ni because $Ni(OH)_2$ was the catalyst precursor species, however high catalytic activity, such as that observed herein, generally originates from incorporation of trace amounts of Fe into the $Ni(OH)_2$ films to form a Fe-Ni oxyhydroxide OER electrocatalyst.[6, 7]

Discussion of time dependence of the Faradaic efficiency and potential of the Pd/C coated Ti mesh cathode

The slight decay of the Faradic efficiency and potential of the Pd/C coated Ti mesh cathode was due to CO poisoning of the catalyst, which can be regenerated by brief exposure to air,[3] but the pH of the electrolyte was maintained at the initial values throughput the experiments by the use of the bipolar membrane.

Calculation of standard error/standard error bar

The standard error was estimated by dividing the standard deviation of data obtained, for three electrodes run under nominally the same conditions, by the square root of sample size. An overpotential of 310 mV was measured at a current density of 8.5 mA cm^{-2}. As shown in Figure 1C, at 10 mA cm^{-2}, the p^+-Si/TiO_2/Ni anode exhibited an overpotential of 320 mV for the OER. The *J-E* behavior of two additional p^+-Si/TiO_2/Ni electrodes was measured, and the overpotential and standard errors were determined to be: 330 ± 10 mV for 10 mA cm^{-2} and 320 ± 7 mV for 8.5 mA cm^{-2}. The Ni overpotential is consistent with prior work that has reported an overpotential of 330 ± 7 mV at 10 mA cm^{-2} under the same Ni fabrication and testing conditions as those used

herein.[8]

Performance characteristics of larger area cathodes and bipolar membranes

The Faradaic efficiency of formate production as a function of time, for -70 mV and -120 mV overpotentials, using a 1 cm^2 Pd/C nanoparticle-coated Ti mesh in CO_2-saturated 2.8 M $KHCO_3$(aq) was similar to that observed for cathode that had a geometric area of 0.04 cm^2 (Figure S5A). The bipolar membrane voltage loss versus current density, normalized to the 0.785 cm^2 bipolar membrane area, was also similar to that observed for a bipolar membrane having a geometric area of 0.03 cm^2 (Figure S5B).

Calculation and discussion of solar-to formate conversion efficiency (η_{STF})

The equilibrium potential for the CO_2/HCO_2^- couple was 0.02 V versus the reversible hydrogen electrode (RHE).[4] Hence, the voltage required for the full chemical reaction, $2OH^- + 2CO_2 = 2HCOO^- + O_2$, was 1.21 V. The solar-to fuels efficiency is defined by:[2, 9]

$$\eta_{solar-to\ fuels} = \frac{J_{op}[\text{A cm}^{-2}] \times E_0[V] \times Faradaic\ efficiency\ of\ fuels\ production}{I_{solar}[W\ cm^{-2}]}$$

where J_{op} is operating current density; E_0 is the voltage required for the full chemical reaction; and I_{solar} is the solar power density.

In this example:

$$\eta_{STF} = \frac{1.21\ \text{V} \times J_{electrode} mA\ cm^{-2} \times Faradaic\ efficiency\ of\ formate}{100\ mW\ cm^{-2}}$$

During the stability test, the overpotential for Pd/C coated Ti mesh cathode was between -40 mV and -100 mV, therefore, as shown in Figure 1B, the Faradaic efficiency of CO_2 reduction to formate was ~100%, 98%, 95%, 94% after 30 min, 1 h, 2 h, 3 h, respectively. The corresponding solar-to formate conversion efficiency was thus 10.5%, 10.3%, 10.0%, and 9.9%, respectively.

Calculation of the area required to collect enough solar photon flux for CO_2 reduction

Consider a coal plant operating 24 hours a day with a CO_2 emission rate of 1400 lb/MWh. Given that the photocurrent density is 8 mA cm^{-2}, and CO_2 is reduced to formate (2-electron process) with an average photocurrent density of 1.6 mA cm^{-2} (20% capacity factor), then for a 100 MW power plant:

The CO_2 emission rate: $\frac{1400\text{lb/MWh}\times 0.4536\text{kg/lb}}{3600\ s/h} \times 100\ MW = 17.64\ \text{kg/s}$

Photocurrent: $\frac{17.64\ \text{kg s}^{-1}\times 1000\ \text{g kg}^{-1}}{44\ g\ mol^{-1}} \times 96500\ C\ mol^{-1} \times 2 = 7.74 \times 10^7 A$

Area: $\frac{7.74\times 10^7 A}{0.0016\ A\ cm^{-2}} * 10^{-4}\ m^2\ cm^{-2} = 5 \times 10^6\ m^2$

Therefore, the required solar photon capture area is on the order of 10^7 m^2.

Tables:

Table S1. Comparison of voltage losses for three cell configurations at $J_{\text{electrode/membrane}}$ = 10 mA cm^{-2}

Components	(Cathode) 2.8 M $KHCO_3$/BPM/1.0 M KOH (Anode)	(Cathode) 2.8 M $KHCO_3$/BPM/2.8 M $KHCO_3$ (Anode)	(Cathode) 2.8 M $KHCO_3$/Nafion Membrane/2.8 M $KHCO_3$ (Anode)
Membrane	0.507 ± 0.038 V	~0.880 V (Figure S8)	0.214 ± 0.015 V
Ni OER overpotential	0.33 ± 0.01 V	0.793 ± 0.026 V	0.793 ± 0.026 V
Pd/C coated Ti mesh CO_2R to formate overpotential	0.057 ± 0.008 V	0.057 ± 0.008 V	0.057 ± 0.008 V
Total voltage loss	~0.89 V	~1.73 V	~1.06 V

Table S2. Comparison of voltage losses for three cell configurations at $J_{\text{electrode/membrane}}$ = 8.5 mA cm^{-2}

Components	(Cathode) 2.8 M	(Cathode) 2.8 M	(Cathode) 2.8 M

	$KHCO_3$/BPM/1.0 M KOH (Anode)	$KHCO_3$/BPM/2.8 M $KHCO_3$ (Anode)	$KHCO_3$/Nafion Membrane/2.8 M $KHCO_3$ (Anode)
Membrane	~0.48 V	~0.82 V (Figure S8)	~ 0.18 V
Ni OER overpotential	0.320 ± 0.007 V	0.783 ± 0.026 V	0.783 ± 0.026 V
Pd/C coated Ti mesh CO_2R to formate overpotential	0.052 ± 0.008 V	0.052 ± 0.008 V	0.052 ± 0.008 V
Total voltage loss	~0.85 V*	~1.66 V	~1.01 V*

*The total voltage loss difference between (Cathode) 2.8 M $KHCO_3$/BPM/1.0 M KOH (Anode) and (Cathode) 2.8 M $KHCO_3$/Nafion Membrane/2.8 M $KHCO_3$ (Anode) configurations was close to 180 mV experimental value.

Figures:

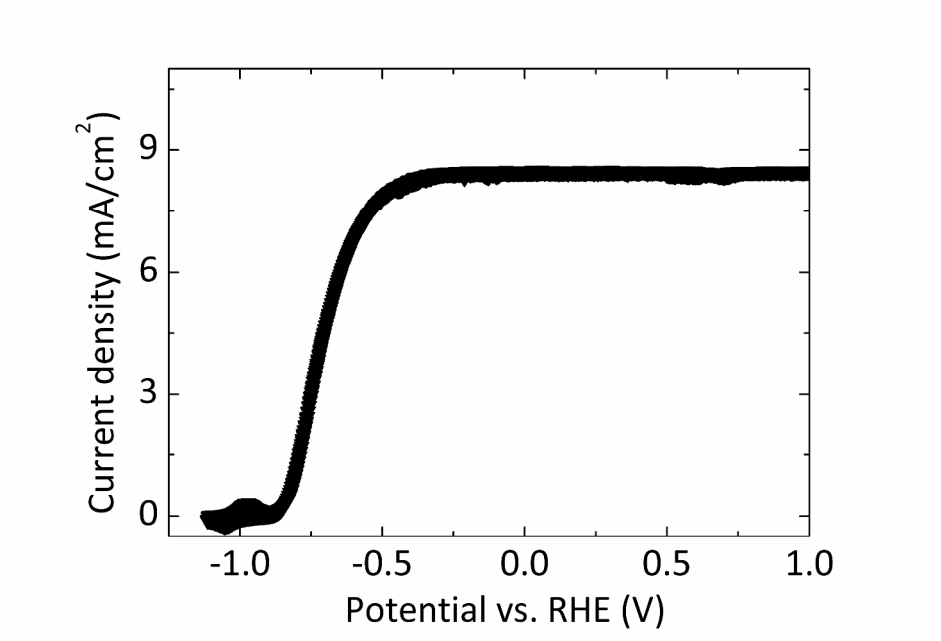

Figure S1. Cyclic voltammetry of GaAs/InGaP/TiO_2/Ni photoanode in 1.0 M KOH(aq) under 100 mW cm^{-2} of simulated AM1.5 illumination.[1]

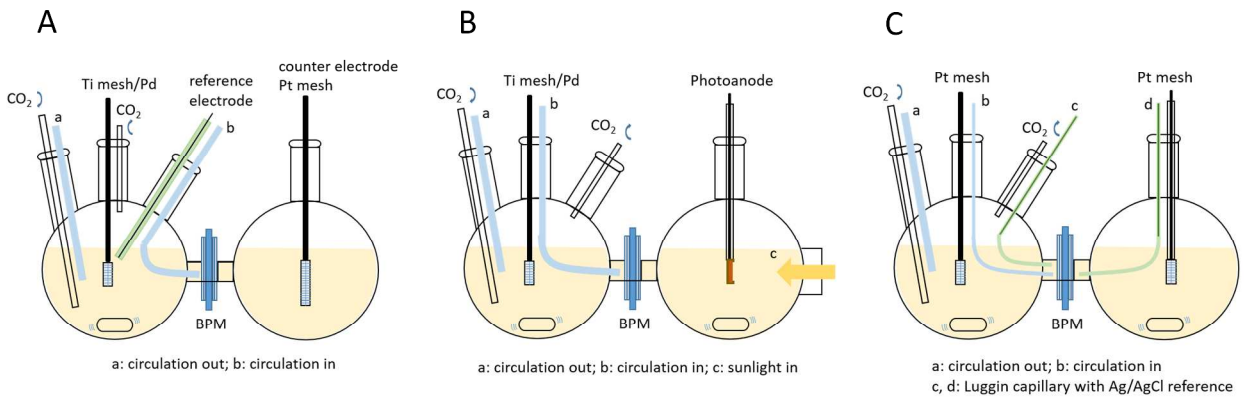

Figure S2. Schematic drawings showing the configuration for 3-electrode (A), 2-electrode (B) electrochemical measurements and the 4-point measurement system for BPM measurements (C).

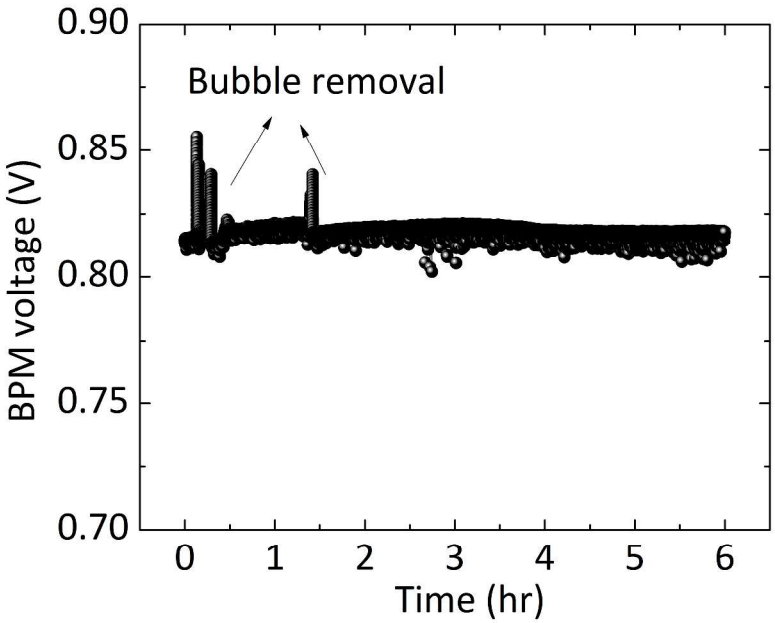

Figure S3. The bipolar membrane voltage as a function of time when the current density through the bipolar membrane was maintained at 8.5 mA cm^{-2}.

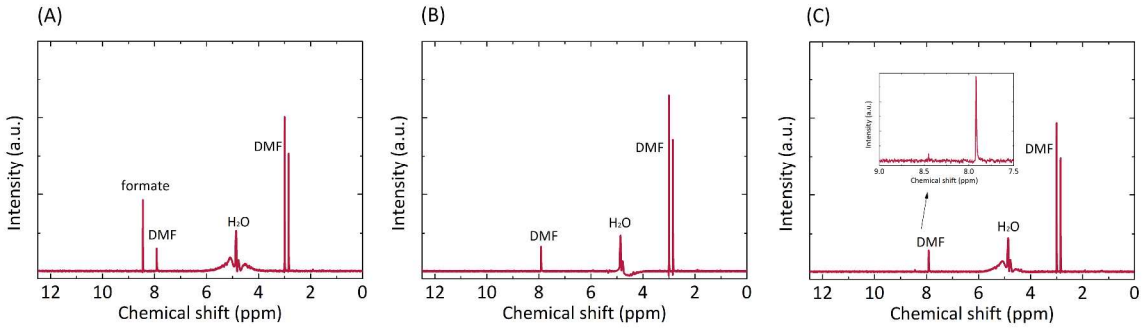

Figure S4. ^{1}H-NMR spectrum of the solutions in the cathode (A) and anode (B) compartments in a 2-electrode electrochemical configuration. Signals at 7.92, 3.01 and 2.98 ppm are the internal standard DMF, while the singlet at 8.44 ppm is formate. The concentration of formate in catholyte was ~ 1 mM, and no formate was detected in the anolyte by ^{1}H-NMR spectroscopy. The membrane area was ~0.03 cm^2, and the membrane current density during operation was 8.5 mA cm^{-2}. The volumes of the catholyte and anolyte were 50 ml and 25 ml, respectively. The operation time was 3 hours. When the concentration of formate in catholyte increased to 0.1 M, and the area of the BPM increased to 0.12 cm^2 (other conditions unchanged), small amount of formate (~ 16 μM) in the anolyte was detected by ^{1}H-NMR spectrum (C) after 3 hours of operation. The current density for formate crossover from catholyte to anolyte was ~30 μA cm^{-2}.

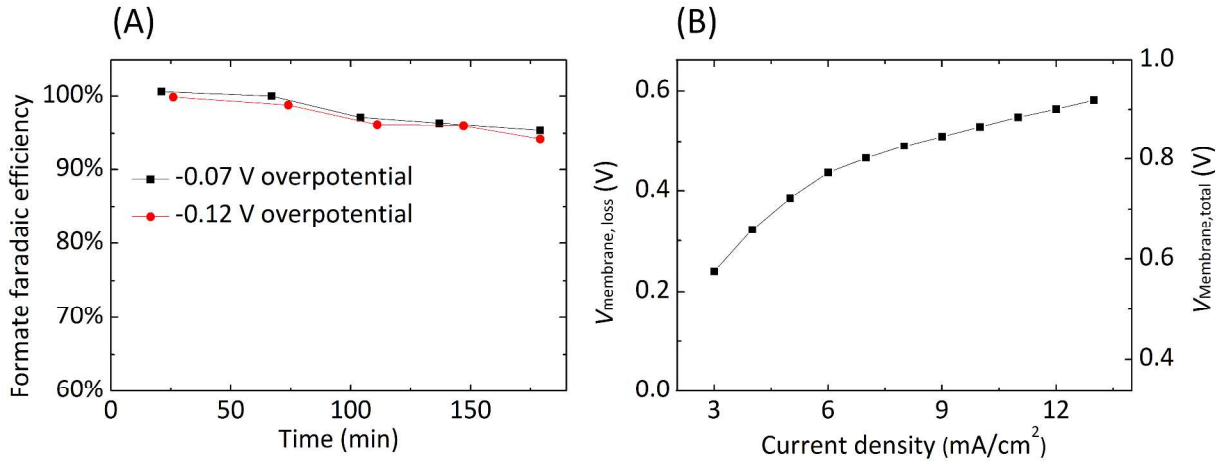

Figure S5. (A) Faradaic efficiency of formate production as a function of time, for -70 mV and -120 mV overpotentials, using 1 cm^2 Pd/C nanoparticle-coated Ti mesh in CO_2-saturated 2.8

M $KHCO_3$(aq). (B) Membrane voltage loss (left axis) and measured total membrane voltage (right axis) as a function of the current density normalized to the 0.785 cm^2 BPM area. The cell configuration was $KHCO_3$(aq) (pH=8.0)/BPM/KOH (aq, pH=13.7).

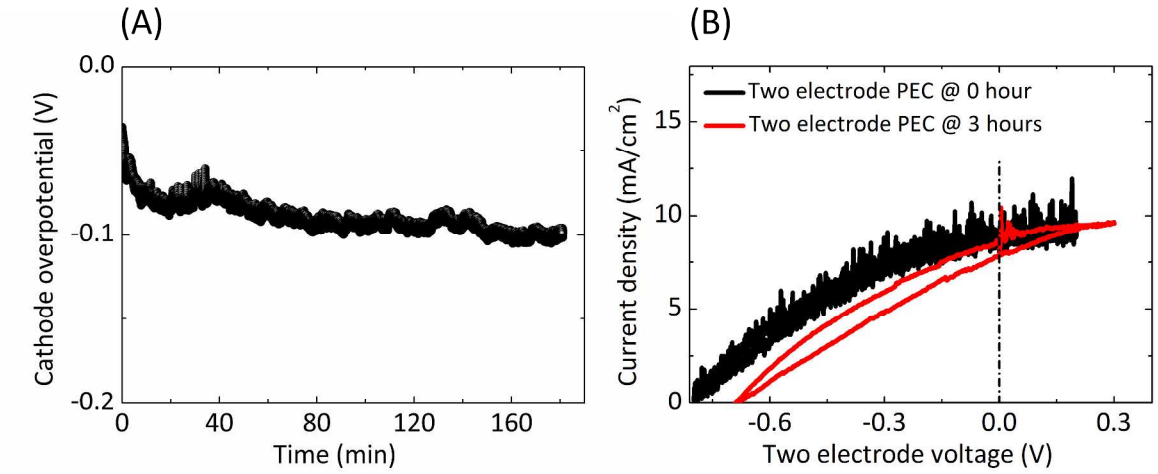

Figure S6. (A) The overpotential for a Pd/C cathode during solar-driven CO_2R using GaAs/InGaP/TiO_2/Ni as a photoanode in a 2-electrode electrochemical configuration under simulated AM1.5 1-Sun illumination. (see p. S9 for discussion about the time dependence of the potential for the Pd/C-coated Ti mesh cathode.) (B) 2-electrode *J-V* behavior with a GaAs/InGaP/TiO_2/Ni photoanode and a Pd/C on Ti mesh cathode in a BPM configuration under simulated AM1.5 1-Sun illumination at 0 and 3 h, respectively, of the stability test.

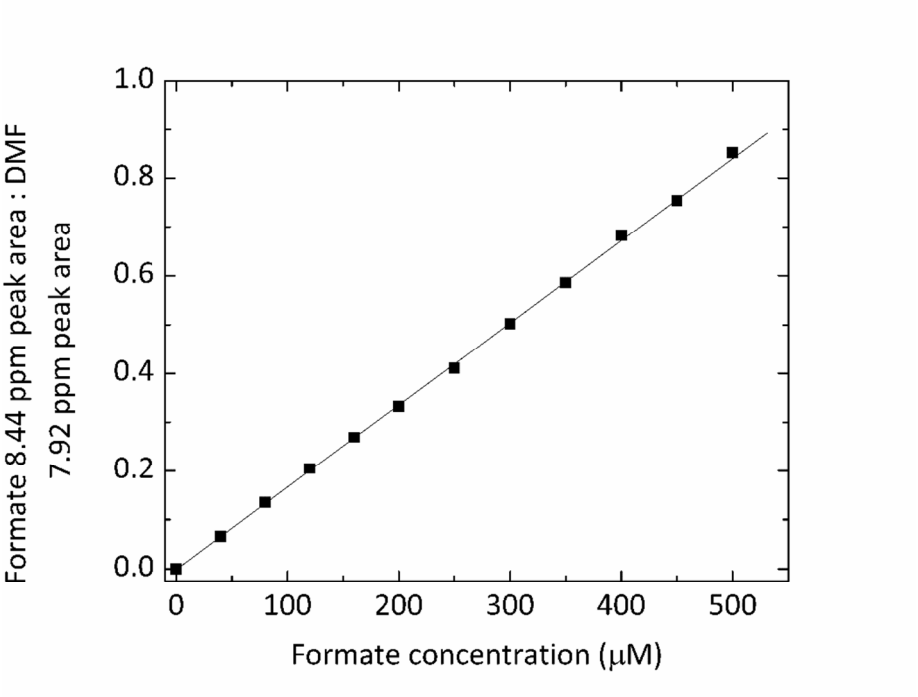

Figure S7. Formate concentration calibration curve: the ratio of the formate 8.44 ppm peak area and the DMF 7.92 ppm peak area as a function of formate concentration. ($R^2 = 0.9996$)

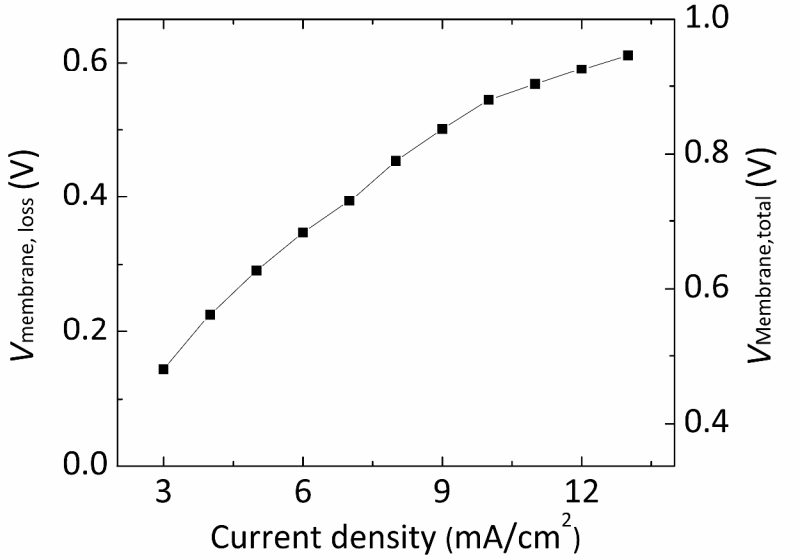

Figure S8. Membrane voltage loss (left axis) and measured total membrane voltage (right axis) as a function of the current density normalized to the 0.030 cm^2 BPM area. The cell configuration was $KHCO_3$(aq) (pH=8.0)/BPM/$KHCO_3$(aq) (pH=8.0).

References:

(1) Verlage, E.; Hu, S.; Liu, R.; Jones, R. J. R.; Sun, K.; Xiang, C.; Lewis, N. S.; Atwater, H. A. A monolithically integrated, intrinsically safe, 10% efficient, solar-driven water-splitting system based on active, stable earth-abundant electrocatalysts in conjunction with tandem III-V light absorbers protected by amorphous TiO_2 films. *Energy Environ. Sci.* **2015**, *8*, 3166-3172.

(2) Coridan, R. H.; Nielander, A. C.; Francis, S. A.; McDowell, M. T.; Dix, V.; Chatman, S. M.; Lewis, N. S. Methods for comparing the performance of energy-conversion systems for use in solar fuels and solar electricity generation. *Energy Environ. Sci.* **2015**, *8*, 2886-2901.

(3) Min, X.; Kanan, M. W. Pd-Catalyzed Electrohydrogenation of Carbon Dioxide to Formate: High Mass Activity at Low Overpotential and Identification of the Deactivation Pathway. *J. Am. Chem. Soc.* **2015**, *137*, 4701-4708.

(4) Kortlever, R.; Peters, I.; Koper, S.; Koper, M. T. M. Electrochemical CO_2 Reduction to Formic Acid at Low Overpotential and with High Faradaic Efficiency on Carbon-Supported Bimetallic Pd–Pt Nanoparticles. *ACS Catal.* **2015**, *5*, 3916-3923.

(5) Sun, K.; Liu, R.; Chen, Y.; Verlage, E.; Lewis, N. S.; Xiang, C. A Stabilized, Intrinsically Safe, 10% Efficient, Solar-Driven Water-Splitting Cell Incorporating Earth-Abundant Electrocatalysts with Steady-State pH Gradients and Product Separation Enabled by a Bipolar Membrane. *Adv. Energy Mater.* **2016**, *6*, 1600379.

(6) Trotochaud, L.; Young, S. L.; Ranney, J. K.; Boettcher, S. W. Nickel–Iron Oxyhydroxide Oxygen-Evolution Electrocatalysts: The Role of Intentional and Incidental Iron Incorporation. *J. Am. Chem. Soc.* **2014**, *136*, 6744-6753.

(7) Corrigan, D. A. The Catalysis of the Oxygen Evolution Reaction by Iron Impurities in Thin Film Nickel Oxide Electrodes. *J. Electrochem. Soc.* **1987**, *134*, 377-384.

(8) Sun, K.; Saadi, F. H.; Lichterman, M. F.; Hale, W. G.; Wang, H.-P.; Zhou, X.; Plymale, N. T.; Omelchenko, S. T.; He, J.-H.; Papadantonakis, K. M.; et al. Stable solar-driven oxidation of water by semiconducting photoanodes protected by transparent catalytic nickel oxide films. *Proc. Natl. Acad. Sci. U.S.A.* **2015**, *112*, 3612-3617.

(9) Schreier, M.; Curvat, L.; Giordano, F.; Steier, L.; Abate, A.; Zakeeruddin, S. M.; Luo, J.; Mayer, M. T.; Gratzel, M. Efficient photosynthesis of carbon monoxide from CO_2 using perovskite photovoltaics. *Nat. Commun.* **2015**, *6*, 7326.